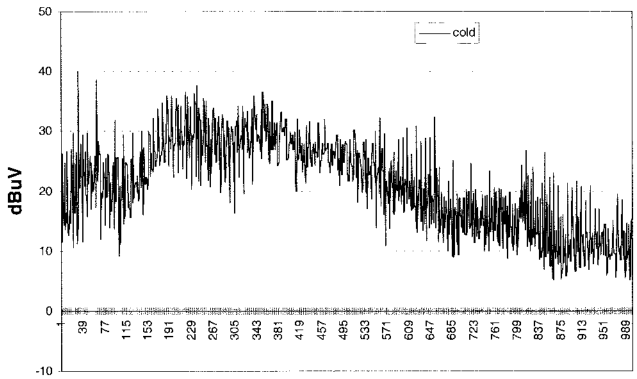

Fig. 24. Spectrum of the HC16 at -40 °C.

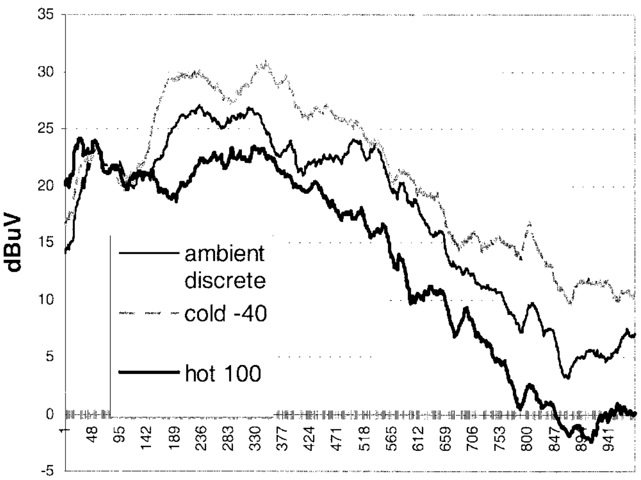

Fig. 25. Spectral emissions as a function of temperature.

into the structure of emissions from VLSI devices and has allowed us to begin building a database. The creation of this database will allow us to be able to compare any and all changes that are made at the device level and at the software level.

Additionally, observation of so many spectrums has enabled us to begin speculating about possible analytical models for describing the emissions from VLSI devices. The measured spectrums are seen to have rapid variations across the measured band. Two explanations come to mind. The first is that the spectrum is a result of an ensemble of pseudorandom binary processes. The second is that the spectrum is the result of an excited two-dimensional electron gas in the underlying substrates of the device. The second explanation is described in the companion paper to this paper. It has the merit that it explains the temperature dependencies of the measured spectrums while the first explanation cannot.

The measured levels of the 16-bit devices are significant for electromagnetic interference. The levels are high enough for coupling to occur between the processor and other regions of the PCB. This has been seen to occur in certain automotive applications. The processor has been seen to be the source of common mode currents that have been coupled to the module I/O connector. These currents in turn, drive the electrical system harness.

Acknowledgment

The authors would like to thank the people at Motorola for their unflinching support given during the gathering of these measurements. They would also like to thank D. Graden and S. Merrill.

References

[1] J. Muccioli, T. North, and K. Slattery, "Investigation of the theoretical basis for using a 1 GHz TEM cell to evaluate the radiated emissions from integrated circuits," presented at *IEEE Int. Symp. Electromagn. Compat.*, Santa Clara, CA, Aug. 1996.

[2] A. Engel, "Model of IC emissions into a TEM cell," presented at *IEEE Int. Symp. Electromagn. Compat.*, Austin, TX, Aug. 1997.

[3] T. DiBene and J. Knighten, "Effects of device variations on the EMI potential of high speed digital integrated circuits," presented at *IEEE Int. Symp. Electromagn. Compat.*, Austin, TX, Aug. 1997.

A Simple Formula for the Ground Resistance Calculation

Sergey L. Loyka

***Abstract*—Simple approximate formulas for the ground resistance and the potential distribution that have quite good accuracy are presented. The use of these formulas can simplify and make faster the calculation of ground path coupling.**

***Index Terms*—Ground-path coupling, ground resistance, potential distribution.**

I. Introduction

A common ground path is a way of coupling between a disturbing source and a victim circuit. This kind of coupling has got a detailed consideration in the literature. The resistance between electrodes and the potential distribution are important quantities for the coupling calculation [1]. The resistance between the two electrodes on a finitely conducting plate of thickness t and of infinite extent is given by [1]

$$R_{ab} = \frac{1}{\pi\sigma}\left[\frac{1}{a} + 2\sum_{n=1}^{\infty}\left\{\frac{1}{\sqrt{a^2+(2nt)^2}} - \frac{1}{\sqrt{d^2+(2nt)^2}}\right\}\right] \tag{1}$$

where a is the electrode radius, d is the separation between the two electrodes, and σ is the plate conductivity. The geometry of the problem is shown on Fig. 1.

As it is pointed out in [1], "...each term in the sum behaves asymptotically as $1/n$ and, consequently, is not strictly summable independently. However, the two terms in the sum, when taken together, fall off faster than $1/n$, and the infinite series converges." To determine the exact degree of the falling off, we bring the two terms in the sum to the common denominator and multiply the numerator and the denominator by the same expression

Manuscript received October 14, 1998; revised February 5, 1999.

The author is with the Swiss Federal Institute of Technology, LEMA-EPFL-Ecublens, Lausanne, CH-1015 Switzerland.

Publisher Item Identifier S 0018-9375(99)04088-0.

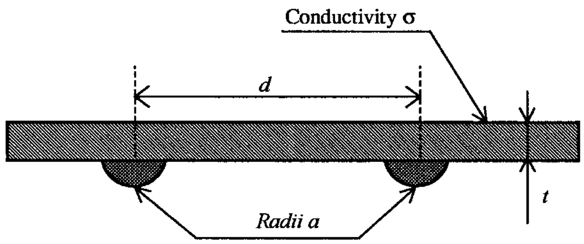

Fig. 1. Two identical hemispherical electrodes of radii a on a lossy infinite plate of thickness t.

$\sqrt{a^2+(2nt)^2}+\sqrt{d^2+(2nt)^2}$ and obtain

$$R_{ab} = \frac{1}{\pi\sigma a}\left[1 + 2a\sum_{n=1}^{\infty}\frac{d^2-a^2}{\alpha\beta(\alpha+\beta)}\right] \tag{2}$$

where

$$\alpha = \sqrt{a^2+(2nt)^2}, \quad \beta = \sqrt{d^2+(2nt)^2}. \tag{3}$$

Using (2) and (3), we see that the expression under the sum in (1) falls off as $1/n^3$.

Unfortunately, there is no closed-form expression for the resulting summation in (1), so a numerical calculation must be used [1]. However, an approximate closed-form expression can be obtained in order to avoid numerical calculations.

II. Simple Formula for the Ground Resistance

An approximate estimation for the infinite series

$$S = \sum_{n=1}^{\infty} F(n) \tag{4}$$

can often be obtained by the substitution of the series by an integral [2, pp. 17–26]

$$S \approx \int_1^{\infty} F(x)\,dx. \tag{5}$$

Here we use this approach to obtain an approximate estimation for (1), substituting the infinite series by the following integral:

$$S \approx \frac{1}{2t}\int_1^{\infty}\left(\frac{1}{\sqrt{\left(\frac{a}{2t}\right)^2+x^2}} - \frac{1}{\sqrt{\left(\frac{d}{2t}\right)^2+x^2}}\right)dx. \tag{6}$$

Using a closed-form expression for this integral [4], we obtain the following simple formula for the ground resistance:

$$R_{ab} \approx \frac{1}{\pi\sigma a}\left[1 + \frac{a}{t}\ln\left(\frac{\sqrt{1+\left(\frac{d}{2t}\right)^2}+1}{\sqrt{1+\left(\frac{a}{2t}\right)^2}+1}\right)\right]. \tag{7}$$

Fig. 2 shows R_{ab} as a function of t calculated by (1) and by (7). As it can be seen from this figure, (7) gives quite a good approximation for R_{ab} for the whole range of t.

III. Approximate Formulas for the Potential Distribution

Simple approximate formulas for the potential distribution can be derived in a similar way. Let us consider, for example, the potential distribution on the bottom of the plate (the excitation circuit is located on the top of the plate) [1]

$$\Phi_{\mathrm{bot}}(x,y) = \frac{I_0}{\pi\sigma}\sum_{n=1}^{\infty}\left\{\frac{1}{\sqrt{r_a^2+[(2n-1)t]^2}} - \frac{1}{\sqrt{r_b^2+[(2n-1)t]^2}}\right\} \tag{8}$$

where

$$r_a = \sqrt{(x+d/2)^2+y^2}, \quad r_b = \sqrt{(x-d/2)^2+y^2} \tag{9}$$

and I_0 is the injected current. The details of geometry are shown on Figs. 3 and 4 or in [1, p. 98].

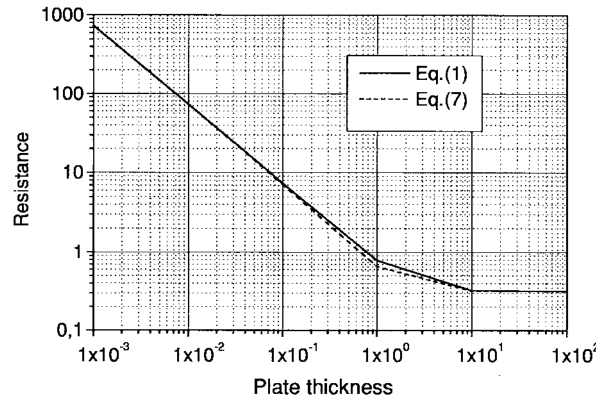

Fig. 2. The resistance between the two electrodes as a function of the plate thickness ($a = 1, d = 10, \sigma = 1$).

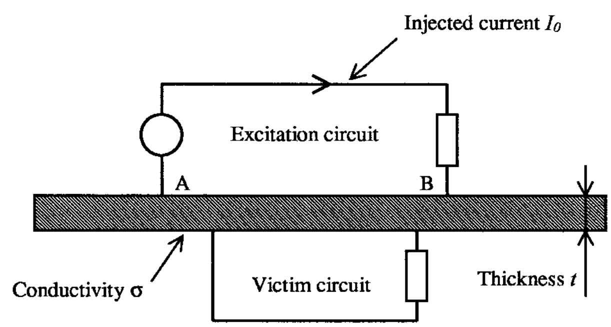

Fig. 3. Excitation circuit—victim circuit coupling on opposite sides of a lossy infinite plate.

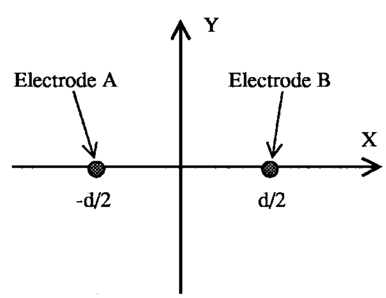

Fig. 4. Coordinate system for Fig. 3.

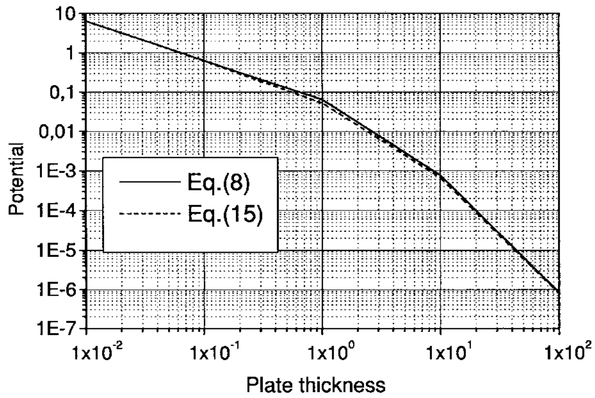

Fig. 5. Potential as a function of the plate thickness ($r_a = 2, r_b = 3, \sigma = 1, I_0 = 1$).

Substituting the infinite series in (8) by an integral similar to (6), we obtain the following approximate expression:

$$\Phi_{\rm bot}(x,y) = \frac{l_0}{2\pi\sigma t}\ \ln\ \frac{\sqrt{1+\left(\frac{r_b}{t}\right)^2}+1}{\sqrt{1+\left(\frac{r_a}{t}\right)^2}+1}. \qquad (10)$$

This formula gives a good approximation for (8) when $t < r_a, r_b$. But, unfortunately, the accuracy of this formula is not very good for $t > r_a, r_b$: the error is about 10 dB. A more accurate approximation of (8) for this case can be obtained in the following manner. Let us transform (8) to the form similar to (2)

$$\Phi_{\rm bot}(x,y) = \frac{l_0}{\pi\sigma}\ \sum_{n=1}^{\infty}\left\{\frac{r_b^2 - r_a^2}{\alpha\beta(\alpha+\beta)}\right\} \qquad (11)$$

where

$$\alpha = \sqrt{r_a^2 + [(2n-1)t]^2}, \quad \beta = \sqrt{r_b^2 + [(2n-1)t]^2}. \qquad (12)$$

For large values of $t(t > r_a, r_b)$, we use the following approximation:

$$\alpha \approx \beta \approx (2n-1)t. \qquad (13)$$

Substituting (13) into (11), after some manipulations we obtain

$$\Phi_{\rm bot}(x,y) \approx \frac{l_0(r_b^2 - r_a^2)}{2\pi\sigma t^3}. \qquad (14)$$

Thus, one can use (10) for small values of $t(t < r_a, r_b)$, and (14) for large values of $t(t > r_a, r_b)$. Fortunately, there is the third possibility: we can correct (10) using (14) and obtain the following formula which has better accuracy for the whole range of t than (10) and (14) used together:

$$\Phi_{\rm bot}(x,y) \approx \frac{l_0}{2\pi\sigma t}\ \ln\ \frac{\sqrt{1+\left(\frac{2r_b}{t}\right)^2}+1}{\sqrt{1+\left(\frac{2r_a}{t}\right)^2}+1}. \qquad (15)$$

(Why so? To arrive to this formula, one should expand the logarithm in (10) into the series of $1/t$ up to the second order and to compare the result with (14) deriving in this way the correction factor for rations r_a/t and r_b/t. Note that this correction does not have any effect for small values of t.) Fig. 5 shows that (15) is in a good agreement with (8) for the whole range of t.

In a similar way, we can obtain an approximation for the potential distribution on the top of the plate [1, (3.87)]).

References

[1] F. Tesche, M. Ianoz, and T. Karlsson, *EMC Analysis Methods and Computational Models*. New York: Wiley, 1997.

[2] Y. B. Zel'dovich and A. D. Myshkis, *Elements of Applied Mathematics*. Moscow, Russia: Nauka, 1967 (in Russian).

[3] I. S. Grandshteyn and I. M. Ryzhik, *Tables of Integrals, Series and Products*. New York: Academic, 1980.

Complex Antenna Factor of a V-Dipole Antenna with Two Coaxial Feeders for Field Measurements

Hisato Hosoyama, Takashi Iwasaki, and Shinobu Ishigami

***Abstract*—In transient field measurements, an antenna with wide-band performance both in amplitude and in phase is desired. The complex antenna factor (CAF) is an appropriate characteristic of such an antenna. It is convenient that the CAF of the wide-band antenna is able to be calculated easily. For this purpose, a V-dipole antenna with a balun consisting of two coaxial feeders is investigated. The calculated complex antenna factors are compared with the measured values. The results show that the V-dipole has the wide-band performance and the CAF is calculable.**

***Index Terms*— Calculable antenna, complex antenna factor, moment method, reference antenna, three antenna method, transient field sensors, V-dipole antenna.**

I. Introduction

In the time-domain measurements of transient electromagnetic fields caused by electrostatic discharges (ESD), the output signal waveform of a sensor is different from the input electromagnetic waveform due to the frequency characteristics of the employed antenna and circuits. The output waveform is represented as a convolution integral of the input waveform and the impluse response of the antenna system. If the impulse response or its Fourier transform (transfer function) can be measured, the input waveform is reconstructed by the deconvolution technique.

As a characteristic of the antenna system, the complex antenna factor (CAF) was proposed [1]. The complex antenna factor, which adds phase values to the conventional scalar antenna factor, is equivalent to the reciprocal of the transfer function. The three antenna method [2] can be used to measure the CAF of any antenna system. However, it requires complicated procedures.

In this paper, a V-dipole antenna with a balun consisting of two coaxial feeders is investigated. The CAF is calculated and compared with the results measured by the reference antenna method.

II. Definition of CAF

When an antenna receives a plane wave as shown in Fig. 1, CAF

Manuscript received January 10, 1998; revised February 26, 1999.

The authors are with the Department of Electronic Engineering, The University of Electro-Communications, Tokyo, 182-8585 Japan.

Publisher Item Identifier S 0018-9375(99)04092-2.